International Journal of Mining Science and Technology 30 (2020) 287–291

Contents lists available at ScienceDirect

International Journal of Mining Science and Technology

journal homepage: www.elsevier.com/locate/ijmst

Multi-phase computer modeling and laboratory study of dust capture by an inertial Vortecone scrubber

Ashish Ranjan Kumar *, Steven Schafrik, Thomas Novak

Department of Mining Engineering, University of Kentucky, 504 Rose Street, 230 Mining and Mineral Resources Building, Lexington, KY 40506, United States

ARTICLE INFO

Article history:
Received 23 October 2019
Received in revised form 18 December 2019
Accepted 24 March 2020
Available online 3 April 2020

Keywords:
Computational fluid dynamics (CFD)
Process safety
Multi-phase flows
Volume of fraction (VOF)
Dust-capture
Cleaning efficiency

ABSTRACT

Dust generated in mining and tunneling activities is hazardous to health of persons and safety of operations. These projects employ pick-milling machines to extract minerals and rock by mechanical breakage. The machines are equipped with flooded-bed scrubbers that encase dust particles within fine water films as particles encounter a flooded wire-mesh screen. A major disadvantage is that the screen gets clogged when particles become trapped within the wire mesh, reducing airflow through the scrubber and increasing ambient dust concentrations. Thus, the system requires frequent maintenance or replacement. The application of a Vortecone scrubber as an improved alternative to conventional fibrous type scrubbers is investigated. A Vortecone forces dust-laden air and water to follow a complex, rapidly swirling motion. The momentum drives dust particles towards the periphery where they are captured by the water film. The operating characteristics of a reduced-scale physical model of a Vortecone, with its primary axis mounted in the horizontal orientation, was analyzed numerically and experimentally. Computational fluid dynamics (CFD) models depicting the spraying action and multi-phase air/water flows using the volume of fraction (VOF) approach, are presented. Experimental results, utilizing an optical particle counting technique to establish the dust-cleaning capabilities of the model, are also described.

1. Introduction

Numerous occupations involve the generation of respirable dust particles, many of which, like coal, silica, and asbestos dust, are known to contribute to respiratory ailments in workers [1–3]. Industries, therefore, have adopted a variety of measures to minimize exposure in the workplace environment [4,5]. However, the problem is aggravated in confined work areas, like underground coal mining operations, where it poses an additional safety hazard. If not diluted to harmless levels, float dust generated in underground coal mines can be transported widely by the ventilating air currents. Coal dust in critical accumulations underground could form an explosive mixture; the explosion at the Upper Big Branch mine in West Virginia, U.S., led to 29 fatalities [6].

In addition to this, miners exposed to coal and silica dust are prone to coal workers' pneumoconiosis (CWP) [7,8]. This is a debilitating ailment resulting in the formation of scar tissue in the lungs, which impedes normal breathing, and has no known cure. Its prevention can be best realized by minimizing the exposure of personnel. Lately, the CWP has seen an upsurge in the Appalachian coal-mining region in the eastern U.S. [9]. Regulatory bodies prescribe threshold exposure limits for dust concentrations [10]. The Federal Coal Mine Health and Safety Act was enacted into law in 1969 and laid down specific provisions to regulate the exposure of miners [11]. The law established exposure limits and called for periodic dust sampling, especially in the designated areas. A NIOSH study in 2008, however, reported an increased occurrence of miners contracting CWP after decades of decline [12]. Subsequently, the "final rule" promulgated in 2014 revised the upper threshold limits of exposure for miners to 1.5 mg/m^3 in coal mines [13].

Ventilating airflow is the mainstay of dust-control strategies, with airflow diluting the concentration of dust particles while directing the particles away from workers [14]. Damage resistant brattice stoppings, air-and-water spray systems, the application of foam, and wetting techniques form the isolation and suppression methods in underground mines [15–18]. Active dust capturing systems, like flooded-bed dust scrubbers, are deployed on continuous mining machines to capture dust generated at the coal face [19]. These scrubbers capture dust particles on a mesh-like impingement screen flooded with water. These systems have proven to reduce respirable dust concentrations between 60% and 90%

* Corresponding author.
E-mail addresses: ashish.kumar@uky.edu, ashi.ismd@gmail.com (A.R. Kumar).

https://doi.org/10.1016/j.ijmst.2020.03.014
2095-2686/

on a mass basis. However, the porous screens are prone to overloading by aerosols and clogging due to deposition of dust particles [20,21]. Therefore, this fibrous screen requires frequent maintenance, which may lead to a loss of machine productivity. Reduced airflow, due to clogging, results in a lowered capture of the dust particles and hence an accompanying higher exposure for workers.

Research efforts at the Institute of Research for Technology Development at the University of Kentucky have led to the development of a Vortecone scrubber (Fig. 1), to capture the oversprayed paint particles on the automobile painting lines [22]. The particle-laden air is accelerated and then discharged into a vortex chamber, resulting in a rapid swirling motion. The heavier particles are differentially cast out of the airstream towards the periphery of the vortex chamber and trapped by the water film. Therefore, trajectories of the particles are altered based on their mass and momentum. Cleaning efficiencies exceeding 99.0% have been realized by the Vortecone with the added benefit of lower power requirements on automobile painting lines. Water used to clean the surface could be recycled and reused for a prolonged period, preventing any transfer of pollutants to other media. The moving water film is continuously replenished, and unlike fibrous screens, clogging is avoided, resulting in a consistent capture of particles.

The authors propose the application of a suitably sized Vortecone as a substitute for the conventional scrubber presently used in the mining industry. A reduced-scale model was used in the experiments to establish the cleaning efficiency of the scrubber. This article presents the flow patterns inside the Vortecone established via steady-state CFD models. Water films in the Vortecone have been modeled using the volume of fraction (VOF) approach. The Lagrangian method of particle tracking is used to mimic the motion of the dust particles in the Vortecone. Finally, laboratory experiments conducted to validate the CFD models are discussed.

2. Computational fluid dynamics modeling

Computational fluid dynamics modeling was used to model the flows inside the Vortecone. This has evolved into a powerful tool to represent flows due to continuous improvements in algorithms and computing resources. It is a finite volume technique where a computer program carries out numerical integration of the equations of continuity, conservation of momentum, and energy by discretization of flow volume. The package, scFLOW, version 14, was used to set up the CFD models [23]. CFD models were generated and laboratory experiments were conducted on a reduced scale model of the Vortecone, measuring about 0.45 m along the primary axis. A 3D drawing of the Vortecone was generated on a CAD platform and imported into scFLOW. All surfaces and the flow volume were registered with unique names. A dense cluster of cubical cells called octree, refined preferentially close to the walls and adapted according to flow parameter gradient, was developed to control the placement of mesh cells in the flow volume. Suitable prism layers were inserted on the solid surfaces, depending on the expected velocities, to capture the boundary layer phenomenon using wall functions.

2.1. Mesh-independence analysis

The mesh-independence study was carried out to develop a computational mesh that was fine enough to capture the flow accurately and to determine its numerical robustness. Three meshes were generated with a progressively higher packing density. The velocity magnitudes at three points–close to the flaps, the curve at the bottom and inside the vortex chamber–were investigated because these locations are important for characterizing the flows. Richardson's method of reporting errors and grid convergence was adopted [24]. Relevant errors were computed using Microsoft Excel Solver. Average relative- and extrapolated-errors were computed to be 0.89% and 0.32%, respectively. The average fine grid convergence index was computed to be 0.53, an excellent value considering the intense circulatory flows inside the Vortecone. The second mesh, with about 2.15 million elements, was used for further analysis, including steady-state, transient-state free-surface modeling, and transient -state particle-tracking and capture.

2.2. Steady-state simulations

Steady-state simulations were first run at different volumetric airflow rates to approximate the associated pressure drops. This also enabled the generation of the pressure-flow plot, known as the system curve. The realizable k-ε turbulence model was chosen for its efficient capabilities in representing flows characterized by high-pressure gradients and recirculation expected in the Vortecone. The volumetric flow rates and associated turbulence properties were defined at the inlet. This included computed values of turbulence kinetic energy and turbulence dissipation rates. Suitable wall functions were imparted on all other surfaces to ensure that the dimensionless normalized wall distance values were not high. The outlet surface was assigned an outflow static pressure value of 0 Pa. Acceleration due to gravity was set at -9.81 m/s^2 along a suitable direction perpendicular to the Vortecone axis. All simulations were run assuming incompressible air as the working fluid. Steady-state simulations with air considered a compressible fluid did not show any significant temperature change. Since all the experiments were run at room temperature (20 °C assigned as initial conditions), any temperature changes due to compressible air would not have resulted in any phase changes in fluids. Removing

Fig. 1. A 3D printed model of the Vortecone developed at the Institute of Research for Technology Development, University of Kentucky.

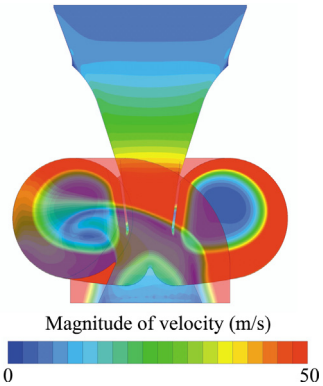

Fig. 2. Contours of velocity magnitude on parallel planes in the Vortecone.

the temperature variable also saved compute time. Fig. 2 shows the contours of velocity magnitude on a plane through the Vortecone when viewed from the top for a flow of 0.38 m^3/s. The steady-state flow regime shows the air moving at much higher speeds at the periphery of the vortex chamber.

2.3. Transient state simulations

A full jet spray, with an outer spray angle of 110°, was incorporated into the laboratory setup to introduce water in the Vortecone. Its geometrical parameters were obtained from the product catalog and included in the CFD models. Because of the enormous computational resources required, two airflows and one water flow through the spray were modeled. The development of water film was represented by transient-state models. Small time-steps of 50.0 and 60.0 μs were used for the flows of 0.38 and 0.28 m^3/s, respectively, to keep the average Courant number under 1.0. This helped to precisely locate the air-water interfaces and dust particles. Small time-steps also prevented any divergence in the solver. Absence of any patterns in the plots of velocity magnitudes at chosen points for a fixed inflow flux and mass flow rates at the outlets obtained from the log files, indicated a flow quickly transitioning into an unsteady turbulent regime in the Vortecone.

The free-surface modeling method using the volume of fraction (VOF) approach was used to track the air-water interface. It is an accurate numerical approach for modeling traveling fronts, including liquid films [25]. Water and dry air were assigned VOF values of 1.00 and 0.00, respectively. All mesh cells with a fractional VOF represent an interface. The water droplets dispensed by the spray were immediately converted to an equivalent VOF. Numerical diffusion of tiny VOFs generated at the spray was prevented by allowing the droplets to coalesce. Fig. 3 shows the films of water, represented by a VOF value of 0.01. The visibly unpredictable shape of the film, after a minimal difference between the inflow and the outflow was observed, is also associated with highly unsteady turbulent flows.

2.4. Particle tracking

The Lagrangian particle-tracking method was used to mimic the motion of dust particles inside the Vortecone. A preliminary analysis of the coal sample yielded a typical diameter range of 0.3–15.0 μm. This study includes particle sizes in the range of 2.0–14.0 μm to enable reliable particle detection. Lower particle sizes were not studied to cover the widest range of particle sizes without running into coincidence errors. Particle diameter and density were fed into the analysis conditions in the CFD software. These particles were randomly released at the inlet of the Vortecone every 0.5 ms for a period of 0.25 s. Simulations were run with five inner iterations for the particle tracking of each cycle. About 98% of the kinetic energy of the particles undergoing a collision with a solid surface is preserved, so a coefficient of restitution of 0.95 was used for all particle-wall interactions [26]. The particles were also programmed to be destroyed at the two outlets. To model the capture of dust particles by the water film, a user-defined formatted script was written and compiled with the solver. The script extracts information about particle position and velocity components along three axes, which were set to 0.00 μm and 0.00 m/s, whenever a particle passes through a mesh cell with an assigned VOF. This resembles particle capture on the liquid surface but not on the solid Vortecone surface. Fig. 4 shows the instantaneous position of dust particles inside the Vortecone at the time, t = 1.25 s. This time was chosen in Fig. 4 because the particle concentration in the Vortecone is maximum at this instance. Beyond this time, particle concentration in the Vortecone begins to decrease since the smaller particles continue to leave the filter uncaptured. The particles are colored by their diameter with red color in Fig. 4 being the largest particles. Iso-surface of volume of fraction has also been shown in Fig. 4, which represents the air-water interface.

The particles reporting at the outlets were counted and sorted into classes based on their diameters. Doing so allowed for estimating the capture efficacies of the Vortecone for the specific diameters of the dust particles. The plot of cleaning efficiency is shown later, along with the laboratory test results.

3. Experiment set-up

Laboratory experiments were conducted on a reduced scale model of the Vortecone. Curved surfaces were generated using a 3D printer, whereas clear polycarbonate sheets were used to construct the flat components of the Vortecone. The Vortecone was installed with its primary axis oriented in the horizontal direction, enabling the injection of air and water perpendicular to gravity at the inlet, as shown in Fig. 5. The Vortecone was installed in series with ductwork measuring 0.30 m × 0.46 m internally. Custom-made transitions and suitable bends with vane and rail arrangements ensured that the pressure drops at the bends were minimal. This also ensured a minimum loss of particles close to the bends later. A centrifugal fan, rated at 18.6 kW and controlled by a variable frequency drive (VFD), was affixed at one end of the duct. An inline, honey-comb, vane-equipped, Dwyer differential station was used to measure total and static pressures. A flow regulator and a digital flow meter were also connected in series to control the inflow of water injected by a full-jet water spray.

An Arduino controlled, stepper motor driven screw feeder was 3D printed for controlled injection of coal dust into the duct and sourced from a small box serving as the dust reservoir. Coal dust was injected into the duct pneumatically. Iso-kinetic sampling was carried out upstream and downstream of the Vortecone to eliminate under-sampling or oversampling of the particle-laden air. Probes were designed and 3D printed to sample the air *iso*-kinetically at 0.28 and 0.38 m^3/s. Two identical optical particle sizers, TSI OPS 3330, were installed upstream and downstream to count and size the particles. Complex refractive index (1.78-0.60i) and density (1220 kg/m^3) values were programmed into the OPS [27]. Deadtime correction was enabled to minimize coincidence errors, especially in smaller particles. The sampled air downstream was first run through a desiccant dryer to remove moisture before being processed by the particle sizer. The differ-

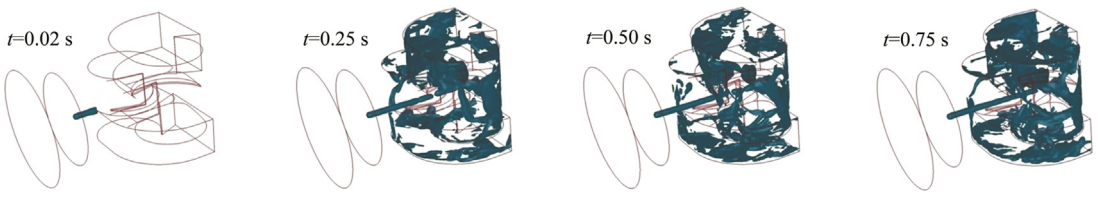

Fig. 3. Iso-surfaces of the VOF value of 0.01 at different instances in time after the fluids move in for airflow of 0.38 m^3/s and water flow being 7.57 l/min.

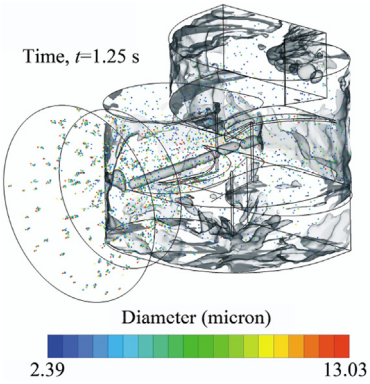

Fig. 4. Position of dust particles colored by their diameter at the time, t = 1.25 s.

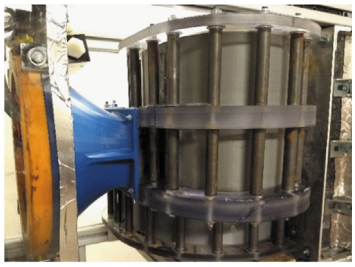

Fig. 5. Mounting the Vortecone with a horizontal orientation.

ence in particle number concentrations obtained from the OPS was converted to equivalent gravimetric concentrations using the TSI aerosol-instrument-manager software. The difference in gravimetric concentrations between the OPSs upstream and downstream yields the cleaning efficiency for particle size range reported by the OPS channels.

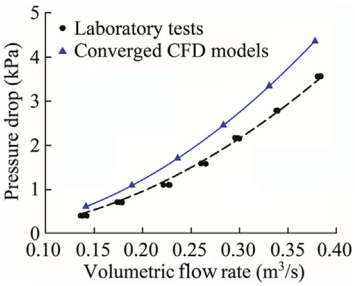

Fig. 6. Flow pressure curves for the experimental set-up.

4. Test procedure

The frequency of the VFD was first set at 15.0 Hz and increased progressively in steps of 5.0 Hz. Corresponding total and static pressures were obtained for all frequencies. Velocity pressures, thus computed, were converted to equivalent volumetric flow rates. Additionally, ductwork was traversed using a hot-wire anemometer to verify the average velocity magnitude and to identify any leakages. A plot of pressure drops, with their associated flows, was generated to obtain the system curve, as shown in Fig. 6. The curve shows a good agreement with the converged steady-state CFD models.

Specific flows could be established through the Vortecone using the generated system curve. The cleaning efficiency of the Vortecone was investigated at the airflows of 0.28 and 0.38 m^3/s. To establish the cleaning efficiency at a known airflow through the system, precisely 5.0 g of coal dust was injected into the ductwork over 8.0 min upstream of the Vortecone using the auger feeder, aided by compressed air. This was done to eliminate coincidence error which could arise due to the sensing volume of the OPS being overwhelmed with too many aerosol particles.

5. Results

Experiments were designed with two different airflows and three water flows, in random order and with three repetitions, to obtain a representative average and to eliminate any systematic errors in testing. Fig. 7 shows the plots of average cleaning efficiency for the two airflows with variation in water influx. The cleaning efficiency of the Vortecone increases with an increase in airflow and the Vortecone traps smaller particles progressively at higher flows. Changes in water inflow rates made small, on a mass basis, changes in particle capture.

A sensitivity analysis of the VOF parameter was carried out by altering the numerical value of the VOF parameter in the user-defined script to mimic the lab testing results. This was done solely for the water flow of 7.57 l/min due to excessive computational resources requirements and small measured changes based on water flow. Fig. 8 shows the plots for the two airflows. A good agreement in the numerical models and laboratory experiments was readily observed under the complex regime of multi-phase flows and particle transportation. A maximum absolute error magnitude of about 9% was observed, which is acceptable under complex multi-phase particle-laden flow regime.

The research investigated the application of the Vortecone scrubber to capture particles that ranged in size 2.0–14.0 μm. This range of particle size is much lower than that of paint particles the Vortecone was initially designed to capture. Experiments show that the Vortecone can capture at least 75% of coal dust particles of size 3.1 μm and above, and 90% or more of particles measuring

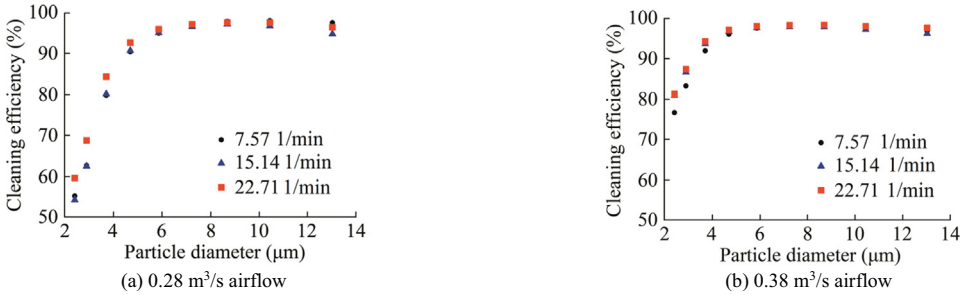

Fig. 7. Plots of cleaning efficiency for airflows of 0.28 and 0.38 m^3/s.

Fig. 8. Sensitivity analysis of the VOF parameter for airflows of 0.28 and 0.38 m^3/s.

5.2 μm at an airflow of 0.28 m^3/s. The cleaning efficiency improves with cut-off diameters falling to 1.9 and 3.2 μm approximately at 0.38 m^3/s. The experiments also show that water flow does not have a significant impact on the cleaning efficiency.

6. Conclusions

CFD models and laboratory experiments show that the Vortecone is an efficient dust scrubber, but it requires a relatively high pressure to sustain required airflows. The numerical models and laboratory tests show that the Vortecone possesses good dust-removal capabilities and could be a favorable alternative to the conventional flooded-bed scrubber presently used in the coal-mining and other industries that deal with aerosols of comparable sizes. The absence of wire-mesh screens, which are prone to clogging, essentially makes the Vortecone scrubber a maintenance-free system.

Computational fluid dynamics (CFD) modeling shows the fluids being accelerated as they travel towards the vortex chamber. The VOF approach applied in the models enables the representation of air-water interfaces developed following the spraying action accurately within acceptable computational time. A particle tracking methodology was adopted to monitor the position of particles inside the Vortecone. Laboratory experiments were also set up where coal dust particles were released into the Vortecone system. Optical particle counting experiment results have agreed with the computer models, and this has established the Vortecone as an efficient system to capture the particles from the airstream to make for a cleaner workplace.

Acknowledgements

This work was supported by the National Institute for Occupational Safety and Health (NIOSH) via Grant 200-2014-59922, "Coal Mine Dust Mitigation through Novel Scrubber Development and Numerical Modeling". The authors also thank Dr. Kozo Saito of the Department of Mechanical Engineering at the University of Kentucky for his invaluable inputs and Oscar Velasquez for setting up the Arduino system.

References

[1] Neuberger M, Westphal G, Bauer P. Long-term effect of occupational dust exposure. Jpn J Ind Health 1988;30(5):362–70.
[2] Meo SA. Health hazards of cement dust. Saudi Med J 2004;25(9):1153–9.
[3] Darcy DJ, Alleman T. Occupational and environmental exposure to asbestos. In: Proceedings of pathology of asbestos-associated diseases. Heidelberg: Springer; 2004. p. 17–33.
[4] Beaudry C, Lavoué J, Sauvé JF, Bégin D, Rhazi MS, Perrault G, et al. Occupational exposure to silica in construction workers: A literature-based exposure database. J Occup Environ Hygiene 2013;10(2):71–7.
[5] Flanagan ME, Seixas N, Majar M, Camp J, Morgan M. Silica dust exposures during selected construction activities. Am Ind Hyg Assoc J 2003;64(3):319–28.
[6] United States Department of Labor. Report of investigation, fatal underground mine explosion. Arlington, Virginia: Mine Safety and Health Administration; 2010.
[7] Borm PJA. Toxicity and occupational health hazards of coal fly ash (CFA). A review of data and comparison to coal mine dust. Ann Occup Hyg 1997;41(6):659–76.
[8] Castranova V, Vallyathan V. Silicosis and coal workers' pneumoconiosis. Environ Health Perspect 2000;108(S4):675–84.
[9] Arnold C. A scourge returns: black lung in Appalachia. Environ Health Perspect 2016;124(1):A13–8.
[10] Occupational Safety and Health Administration. Regulations (Standards- 29 CFR); 2016.
[11] United States Department of Labor. Federal Coal Mine Health and Safety Act of 1969.
[12] Division of Respiratory Disease Studies, NIOSH. Work-Related Lung Disease Surveillance Report. Morgantown, WV: Centers for Disease Control and Prevention, National Institute for Occupational Safety and Health; 2008.
[13] United States Department of Labor. Lowering Miners' Exposure to Respirable Coal Mine Dust, including Continuous Personal Dust Monitors; Final Rule; 2017.
[14] Kissell FN. Handbook for dust control in mining. Pittsburgh, PA: US Department of Health and Human Services, Public Health Service, Centers for Disease Control and Prevention, National Institute for Occupational Safety and Health, Pittsburgh Research Laboratory; 2003.
[15] Timko RJ, Thimons EJ, Min J. Damage-resistant brattice support stoppings in mines with large entries. Eng Min J 1987;188(5):34–6.
[16] Prostański D. Use of air-and-water spraying systems for improving dust control in mines. J Sustainable Min 2013;12(2):29–34.
[17] Wang Q, Wang D, Wang H, Han F, Zhu X, Tang Y, et al. Optimization and implementation of a foam system to suppress dust in coal mine excavation face. Process Saf Environ Prot 2015;96:184–90.
[18] Cybulski K, Malich B, Wieczorek A. Evaluation of the effectiveness of coal and mine dust wetting. J Sustainable Min 2015;14(2):83–92.
[19] Campbell JAL, Moynihan DJ, Roper WD, Wilis EC. Dust control system and method of operation. USA: Patent 4380353; 1983.
[20] Kasper G, Schollmeier S, Meyer J. Structure and density of deposits formed on filter fibers by inertial particle deposition and bounce. J Aerosol Sci 2010;41(12):1167–82.
[21] Agranovski IE, Shapiro M. Clogging of wet filters by dust particles. J Aerosol Sci 2001;32(8):1009–20.
[22] Salazar AJ, Saito K, Alloo RP, Tanaka N. Wet scrubber and paint spray booth including the wet scrubber. USA: Patent 6093250; 2002.
[23] Cradle-CFD: MSC Software Company. Product and Services: scFLOW Features; 2017.
[24] Celik IB, Ghia U, Roache PJ, Freitas CJ, Coleman H, Raad PE. Procedure for estimation and reporting of uncertainty due to discretization in CFD applications. J Fluids Eng, Trans ASME 2008;130(7):0780011–780014.
[25] Hirt CW, Nichols BD. Volume of fluid (VOF) method for the dynamics of free boundaries. J Comput Phys 1981;39(1):201–25.
[26] Tsai C, Pui DYH, Liu BYH. Capture and rebound of small particles upon impact with solid surfaces. Aerosol Sci Technol 1990;12(3):497–507.
[27] McCartney JT, Ergun S. Optical properties of coal and graphite. US Department of the Interior, Bureau of Mines; 1967.